Application of cellular automata to modelling competitive growths of two underwater species *Chara aspera* and *Potamogeton pectinatus* in Lake Veluwe

Q. Chen *, A.E. Mynett, A.W. Minns

Delft Hydraulics, PO Box 177, 2600 MH Delft, The Netherlands

Abstract

The objective of this research is to explore the relatively new approach, cellular automata (CA), to model the competitive growths and then try to explain the succession process of two underwater species *Chara aspera* (*C. aspera*) and *Potamogeton pectinatus* (*P. pectinatus*) in a eutrophicated lake, the Netherlands. CA constitutes a mathematical system that simulates the dynamics of spatial-temporal patterns in discrete steps according to prescribed local evolution rules. It consists of three main components: a set of cells, cell properties or states, and local evolution rules. Comparing to conventional aggregated-based ecological models formulated by partial differential equations (PDE), CA has more flexibility to implement the individual property differences and local interactions, especially with the facilitation of the object-oriented programming (OOP) techniques. The model results are seen to be both qualitatively and quantitatively in agreement with field observations. Namely, CA is not only applicable to ecohydraulics modelling, but also in some aspects more efficient than PDE based models. © 2002 Elsevier Science B.V. All rights reserved.

1. Introduction

Aggregated-based ecological models have been well developed in the past several decades (Dahl-Madsen and Strange-Nielsen, 1974; Chen and Orlob, 1975; Jørgensen, 1976, 1994, 1998; Babovic and Baretta, 1996). These kind of models lump species into biomass and formulate the dynamics into PDE form, e.g. Lotka–Volterra model for description of prey–predator system (see May, 1976). However, this approach fails to reproduce realistic results where differences of individual properties and local interactions play a significant role in determining the relationship between populations, and between species and its their surroundings. As an alternative, the studies of cellular automata based model and spatially explicit individual-based model (IBM) are drawing more attentions from the ecological modelling community.

* Corresponding author. Tel.: +31-15-285-8915; fax: +31-15-285-8582.

E-mail address: qiuwen.chen@wldelft.nl (Q. Chen).

The IBM expresses the population dynamics by describing the individuals and the messages passing between them to trigger appropriate behaviours. It has been widely used in modelling of fish and forest dynamics, and is expected to be a promising ecological model paradigm in the coming years (Hong et al., 1999; Masahiko et al., 1991; DeAngelis and Gross, 1992). Several important research teams including Oak Ridge National Laboratory, Applied Ecology in University of Amsterdam, and Institute for Forestry and Nature Research in University of Wageningen are heading for the applications of IBM. Current research activities include prediction of density-dependent dynamics of smallmouth bass population (DeAngelis and Godbout, 1991), super-individuals for modelling large populations (Scheffer et al., 1995), modelling of marine fish early life history (Hinckley et al., 1996), modelling of predator–prey functional response (Blaine and DeAngelis, 1997), experts system of animal foraging simulation (Carter and Finn, 1999), modelling of juvenile salmon migrating (Petersen and DeAngelis, 2000), modelling of lake fish communities (McDermot and Rose, 2000). However, they are still at the theoretical and analytical stage, besides, the integration with underlying physical processes is not well explored (Anderson, 1995; Donaghay and Osborn, 1997; Chapra, 1998).

The CA based models attempt to reproduce the spatial-temporal dynamic patterns by some simple local evolution rules. A well-known example is Coway's game of life (see, Minns et al., 2000). Recent research in CA and its applications to ecosystem on a large scale includes: the evolution of urban land-use patterns (Engelen et al., 1998), forest fire spreading (Karafyllidis and Thanailakis, 1996), vegetation cover dynamics (Balzter et al., 1997), rainforest dynamics (David

and Ricard, 2000) and so forth. In smaller scale, recent studies have included population dynamic of animals (Gronewold and Sonnenschein, 1998; Sirakoulis et al., 2000), spreading of phytoplankton species (Babovic and Baretta, 1996). Some other applications include patchiness analysis of marine species (Hal and Ron, 1996) and prey–predator system dynamics (Minns et al., 2000).

Comparing to aggregated-based models, both IBM and CA models have obvious flexibility to implement individual property differences and local interactions. The main difference is that IBM takes individual species as study object, while CA model schematise the investigated space into cells and takes each individual cell as study object.

This paper is to present the application of CA to modelling the competitive growths and then explaining the successions of two underwater species *Chara aspera* and *Potamogeton pectinatus* in a eutrophicated lake, the Netherlands. In Section 2, it gives a general introduction about the basic concepts of cellular automata and its system behaviours. Then in Section 3, it describes the case study in Lake Veluwee, the Netherlands. Section 4 presents the model output analysis and ecological explanation for the fact that *C. aspera* finally outcompeted *P. pectinatus*. At the end, the paper discusses the applicability of CA to ecological modelling, and the higher efficiency of CA models over PDE based models in some aspects.

2. Cellular automata

Cellular automata constitute a mathematical system, in which many simple components act together to produce complicated patterns of behaviour. They often exhibit 'self-organisation' behaviour. Even starting from complete disorder, their irreversible evolutions can spontaneously generate an ordered structure.

A cellular automata system usually consists of a regular lattice of sites (cells or automaton). Each site has some properties that are updated in discrete time steps according to local evolution rules ϕ, which are functions of the states of cell itself and its neighbours. Fig. 1a,b illustrate a one-dimensional and a two-dimensional CA system with
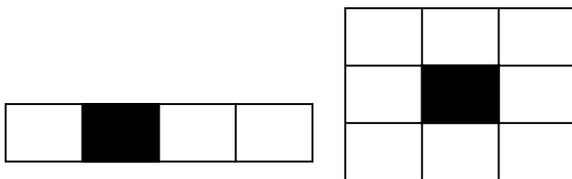
Fig. 1. (a) One-dimensional CA. (b) Two-dimensional CA.
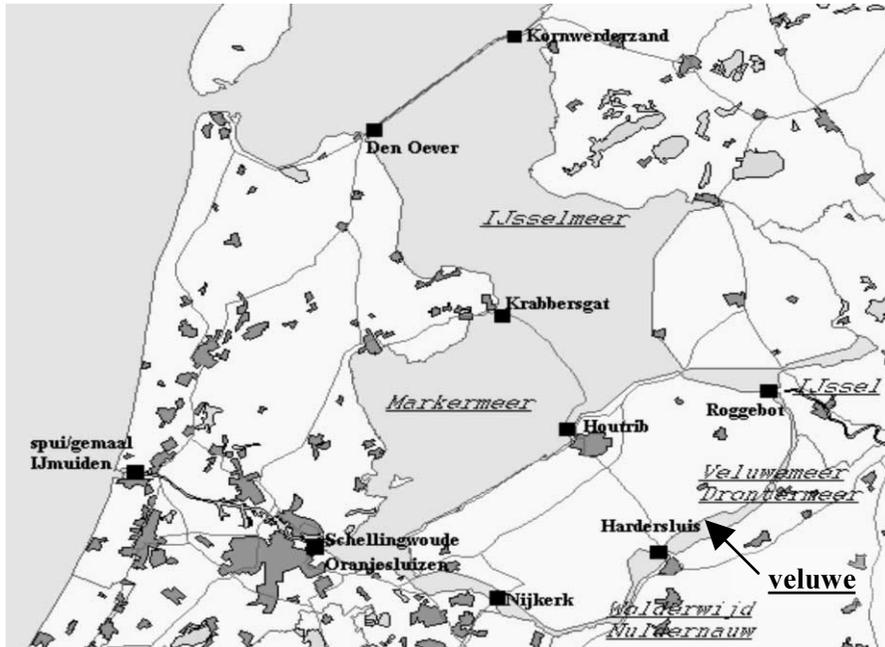
Fig. 2. Location of lake Veluwe, the Netherlands.

the nearest neighbours respectively. The corresponding evolution rules are expressed as Eqs. (1) and (2).

$$a_i^{t+1} = \phi(a_{i-1}^t, a_i^t, a_{i+1}^t) \tag{1}$$

$$a_{i,j}^{t+1}$$

$$= \phi(a_{i,j}^t, a_{i-1,j-1}^t, a_{i-1,j}^t, a_{i-1,j+1}^t, a_{i,j-1}^t, a_{i,j+}$$

$$1^t, a_{i+1,j-1}^t, a_{i+1,j}^t, a_{i+1,j+1}^t) \tag{2}$$

According to the definition, a CA system can be characterised as:

1. Parallelism, which means all cell states are updated simultaneously;
2. Homogeneity, which says that all cells follow the same evolutions rules;
3. Locality, which implies a cell can only gather information from its near neighbours and can only affect its direct neighbours.

First proposed by Von Neumann (1949), the theory and application of CA developed very slowly. This situation was changed after the contribution of Wolfram (1984) to the theoretical construction of CA. However, the trend has been only to investigate simple architectures that pro-

duce complex overall behaviours. Perhaps the best known example is Conway's 'Game of Life'.

The recently increasing use of CA in ecological modelling is motivated by the demand of localised modelling (Babovic and Baretta, 1996; Minns et al., 2000), and is facilitated by the rapid development of object oriented programming (OOP) since it is easy to implement differences of individual properties and local interactions.

3. Case study in Lake Veluwe

3.1. Background of Lake Veluwe

Lake Veluwe is an artificial isolated part of a large Lake IJssel in the centre of the Netherlands. The total water surface is around 3300 ha, with an averaged depth of 1.4 m. It was formed by the construction of dams in the south-east part of the Lake IJssel in 1952 (Fig. 2). According to long-term documentation, the submerged vegetation of the lake has experienced a great change after its formation due to the change of nutrient loading

(Marcel, 1999). Before 1968, the water in the lake was clear, with diverse macrophyte vegetation. Due to discharge of wastewater from some small cities, the lake was eutrophicated, and blue alga became dominant species (Hosper, 1997). Some restoration measures were taken in late 1970s, which resulted in the increase of *P. pectinatus*. The increase of *P. pectinatus* provided the precondition for the return of *C. aspera*. After 1990, *C. aspera* colonised steadily and gradually replaced the dominance of *P. pectinatus*.

From an ecological point of view, it seemed that *P. pectinatus* would outcompete *C. aspera* in this lake system, since: (1) *P. pectinatus* has better ability than *C. aspera* to live in moderate turbid water; (2) *P. pectinatus* germinates earlier and colonises the upper layer, which shade *C. aspera*. In the Lake Veluwe, (3) *P. pectinatus* is less sensitive to eutrophication level, especially to phosphorus concentration, than *C. aspera*. However, *C. aspera* outcompeted *P. pectinatus* and replaced it gradually in Lake Veluwe. Analysis of long-term observations indicated a self-reinforcing ability of *C. aspera* during eutrophication. *C. aspera* returned at a lower phosphorus level (0.1 mg/l) than the level at the time of their disappearance (0.3 mg/l), a phenomenon known as hysteresis (Hosper, 1997; Marcel, 1999), therefore phosphorus is not a key factor in this case. It is supposed that the competition of dissolved inorganic carbon HCO_3^{-1} and competition of light are the two main factors of the succession. However, the replacement process is still unclear, which emerged the demand of model simulation. Considering the environmental heterogeneity and the local interactions, this research selected CA approach to simulate the competition of light and HCO_3^{-1}, and in turn try to explain the replacement process somehow.

3.2. Model structure and main assumptions

The model is designed to contain two partly linked parallel submodels, one for *P. pectinatus* and the other for *C. aspera*. The processes considered in each submodel include shading, attenuation, HCO_3^{-1} competition, photosynthesis, respiration, morality and spreading. A conceptual framework of the model is presented in Fig. 3, where solid lines refer to mass or energy flow, and dash lines mean related processes. The local interactions between the two species are indicated by the two-directions dash lines, for instance 'shading' in Fig. 3.

Before model construction, some important assumptions are made for simplification, which include:

- the spatial scale is $10*10$ m^2, and the temporal scale is 1 day;
- the model lumped vegetation in each cell into biomass, which is counted by ash free dry weight (AFDW);
- the whole depth is considered as one layer since Veluwe is a shallow lake with very little stratification;
- within a day, the irradiation is assumed to be constant in daytime;
- since *C. aspera* and *P. pectinatus* colonise at different vertical positions, different depths are used when computing light attenuation;
- outside well-vegetated area, light attenuation coefficient is constant in the whole growing period. Inside vegetated area, both species have the same attenuation value at first, but after *P. pectinatus* reaches water surface, it takes smaller value than *C. aspera*;
- in the first month after the end of initialisation of *C. aspera*, the concentration of HCO_3^- is the same everywhere, after that, it decreases to 0.4 mM in vegetated area, while remains 2.5 mM outside;
- resources for growth are allocated after fulfilment of respiration;
- respiration is proportional to current total biomass;
- mortality is also proportional to current total biomass;
- biomass loss due to wave action is neglected;
- grazing effect on biomass loss and propagules dispersal is negligible (Hosper, 1997);
- the saturated biomass density is 350 g AFDW/m^2 (Marcel 1999) for both species;
- a cell is considered as vegetated when 75% saturated biomass is reached;
- spreading happens when the cell is saturated and there is space available in the adjacent eight cells;

- the loss of propagules during winter is a proportion of the total ropagules in the cell.

Some other assumptions are not provided here, which can be found in Appendix A.

3.3. Evolution rules

Unlike stochastic CA models (Minns et al., 2000; David and Ricard, 2000), deterministic evolution rules are used in this CA model. Most of these rules are based on laboratory experiments (Marcel, 1999), and others are regressions of real observation data. General procedures of the model are given in the following section, and the detail algorithms will be presented in Appendix A.

1. germination of *P. pectinatus* and *C. aspera* from propagules;
2. initialisation with exponential growth rate;
3. growing and spreading, which involve the computation of shading coefficients, net light level after shading, underwater light intensity after attenuation, HCO_3^{-1} coefficients, photosynthesis production, biomass loss due to respiration and mortality, resource bulk after subtracting the biomass loss, updating of biomass density, and finally the spreading. These procedures are repeated until the end of growth period;
4. by the end of each life cycle, propagules are produced, which is proportional to the current biomass.

4. Model outputs analysis

The output of the model is presented in two ways. One is the visualisation of growing and spreading patterns of the two species in the lake. Two graphs representing *P. pectinatus* and *C. aspera* respectively show the change of biomass

Fig. 3. Conceptual framework of the model.
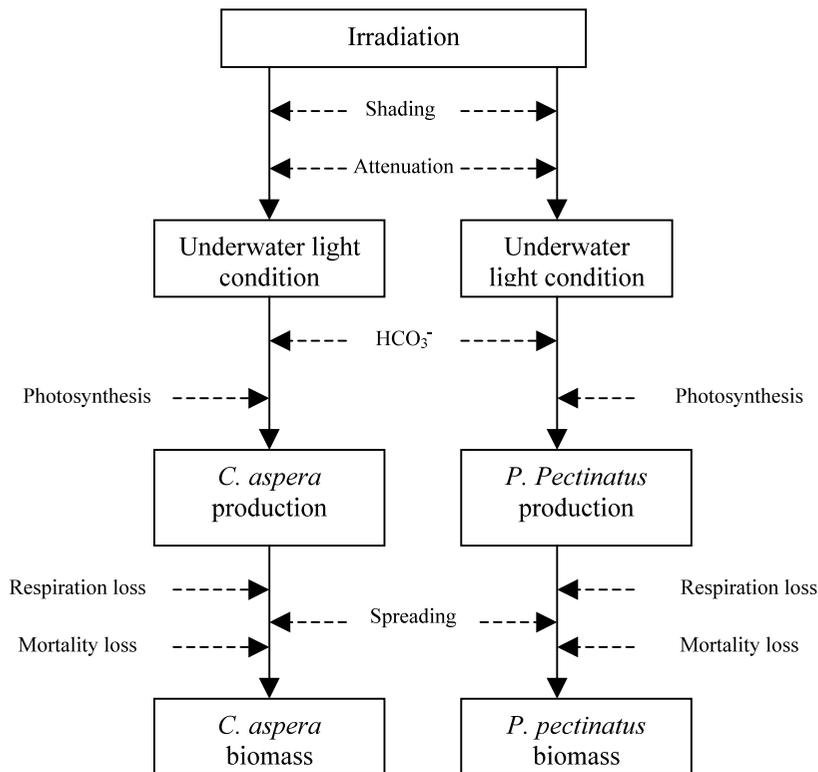
(a)　　　*C. aspera*　　　*P. pectinatus*　　　*C. aspera*　　　*P. pectinatus*　　(b)
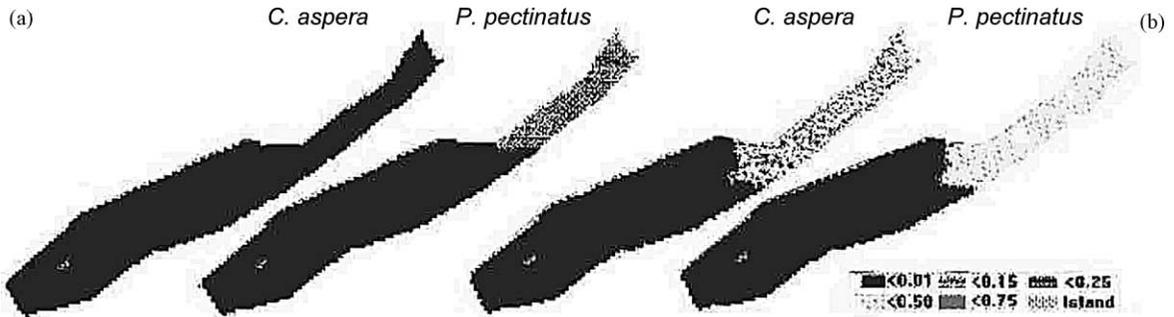
Fig. 4. (a) Germination of both species (*P. pectinatus* germinates earlier than *C. aspera*). (b) Colonisation pattern by the end of the second year (*P. pectinatus* spreads slower than *C. aspera*).

density in each cell and the colonisation process as well (Fig. 4a,b). The other output is a time series of biomass density that is the average of sampled cells (Fig. 5a,b).

As shown in Fig. 4a,b, the colonisation is from the Northeast to the Southwest, and it is faster in longitudinal direction than in transverse direction. Besides, the colonisation of *C. aspera* is faster than that of *P. pectinatus*.

Fig. 5a,b present the annual growth patterns of both species under constant saturated $[HCO_3^{-1}]$ and varying $[HCO_3^{-1}]$, respectively. From the graphs, it can be seen that: in case 1, when keep the HCO_3^{-1} saturated (Fig. 5a), which means no HCO_3^{-1} effect, the growth curves of both species have a similar shape. They grow very slowly at the beginning, then very quickly when irradiation becomes stronger. After that, they reach a stable state. The earlier germination of *P. pectinatus* makes it outcompete *C. aspera* because of shading. Also due to shading, the biomass density of *C. aspera* cannot reach saturation.

In case 2, when $[HCO_3^{-1}]$ decreases following the increase of consumption, the growth curves of both species are quite different from case 1. The earlier germination of *P. pectinatus* makes it contain the growth of *C. aspera* by shading effect, so the biomass density of *C. aspera* is lower than that of *P. pectinatus* at the beginning. Following the increase of biomass and then associated increasing consumption of HCO_3^{-1}, HCO_3^{-1} becomes gradually scarce, which leads to the decline of growth rate of *P. pectinatus*. As the result, *C. aspera* keeps on growing and reaches a high den-

sity due to the relief of shading from *P. pectinatus* at upper layer. Therefore, when HCO_3^{-1} is scare, *C. aspera* outcompetes *P. pectinatus*.

Comparing the two growth curves of *C. aspera* under different $[HCO_3^{-1}]$, it can be seen that *C. aspera* grows better under relatively low $[HCO_3^{-1}]$ situation. Although the scarcity of HCO_3^{-1} also has a negative effect on *C. aspera* growth, the decline of *P. pectinatus* growth due to lack of HCO_3^{-1} has much greater positive effect. Since *P. pectinatus* grows at upper layer, the decline will greatly increase light penetration, which stimulates *C. aspera* to grow.

Comparing the two growth curves of *P. pectinatus* under different $[HCO_3^{-1}]$, it is found that *P. pectinatus* can not grow well under low $[HCO_3^{-1}]$ situation although it contains the growth of *C. aspera* at the early stage. The decline of *P. pectinatus* greatly relieves the shading effects, so that the growth of *C. aspera* is encouraged.

For both species, the two growth curves under different $[HCO_3^{-1}]$ are similar at the early stage. The reason is that the growths at the beginning are very slow, so that the HCO_3^{-1} effects are not obvious.

Generally speaking, the light intensity and HCO_3^{-1} are two major factors to the competitive growths of *C. aspera* and *P. pectinatus* in Lake Veluwe. The scarcity of HCO_3^{-1} has a great negative effect on the growth of *P. pectinatus*, while it has a great indirect positive effect on the growth of *C. aspera*, which is advantageous to the replacement of *C. aspera* to *P. pectinatus*.

5. Conclusions and discussions

The results above manifest that the colonisation is from the Northeast to Southwest, and the spreading is faster in longitudinal direction than in transversal direction. HCO_3^{-1} and light intensity are observed to be two major factors of the system and in turn that shading and competition of HCO_3^{-1} become two important processes. These results are compatible with the field observations (Marcel, 1999) and those from Van Nes et al. (1998), who explored an individual based model to study the effects of changing environmental conditions on the dynamics between *C. aspera* and *P. pectinatus*.

It can be seen from the case study that CA based model shows higher efficiency than PDE based models (Vermij, 1987; Elisabeth, 1992) regarding the implementation of individual property differences, local interactions and discrete process. For instance, it is easy to incorporate the local internal and external interactions such as shading
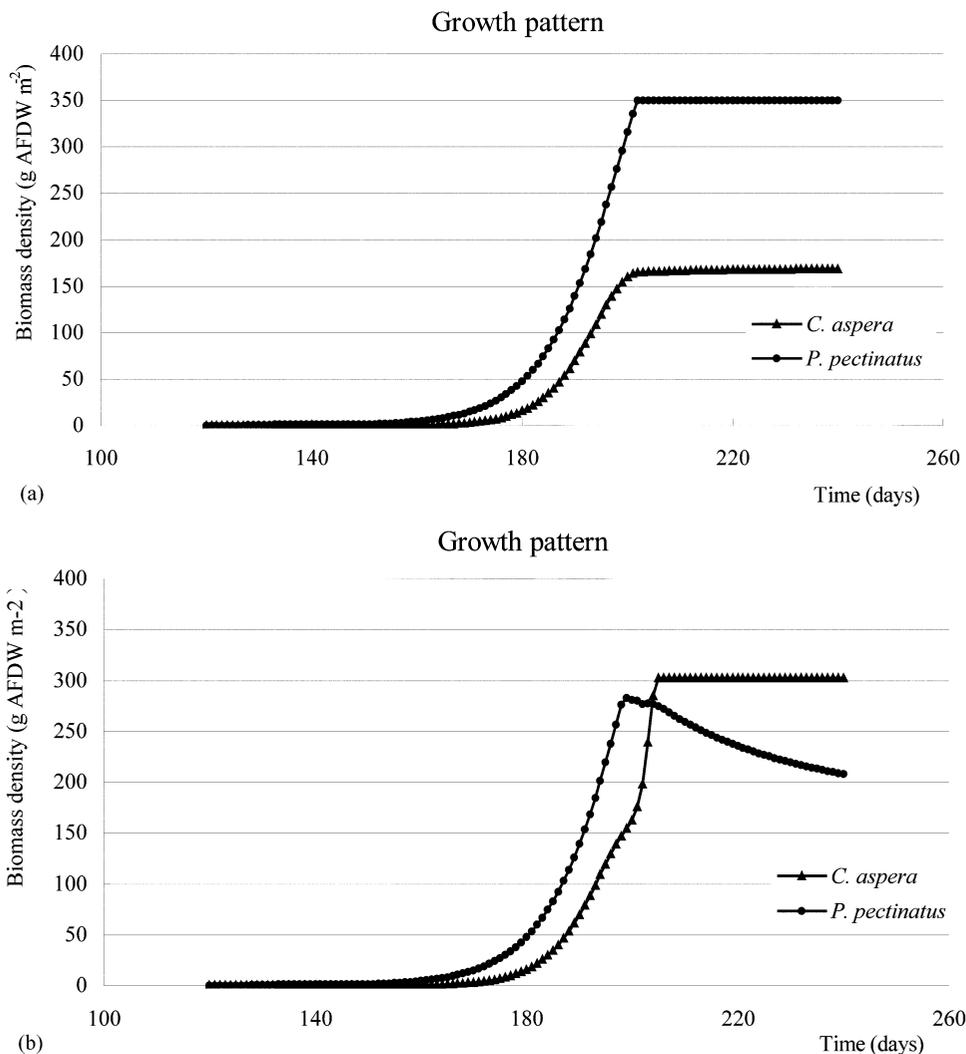
Fig. 5. (a) Yearly growth pattern (under constant saturated $[HCO_3^{-1}]$ condition). (b) Yearly growth pattern (under varying $[HCO_3^{-1}]$ condition)

and HCO_3^{-1} competition for each cell. It is also convenient to specify the differences of individual properties, e.g. vegetated or non-vegetated status, non-uniform distribution of propagules. The computations were carried out in a discrete way by difference equations (not differential equations), which is more realistic from an ecological point of view. All these advantages are especially enhanced when using OOP technology, where a cell can be considered as an object, cell properties as member variables, and interactions as member functions.

Due to the spatial heterogeneity of environmental conditions and the adaptation of species to environment changing, different evolution rules should be applied in different cells. Although it is practical (Camara et al., 1990; Rechnagel et al., 1994) with current available computation capacity, it is not realised in this study. The same as other CA based ecological models from literatures, cells with unique size and geometry are also used in this study, which is quite arguable. Finally, the definition of appropriate evolution rules becomes very difficult because of high complexity and non-linearity when more details are included.

Therefore, our further studies on the application of CA to ecohydraulics modelling include (1) incorporating hydrodynamic module output as forcing dynamics to ecological models. A potential problem is the multiple temporal-spatial scales coupling between hydrodynamic process and ecological process; (2) considering the heterogeneity of evolutions rules. It is better to cluster the studied area, and then apply different rules to different class; (3) schematise the studied space into unstructured cells with different size and geometry according to their environmental or ecological characteristics. Although it violates the original definition of CA, it has better perspectives not only with respect to the ecological reality, but also to the coupling with real observations and computation efficiency; (4) conventionally, the evolution rules are formulated by PDEs, such as Lotka–Voterra equations in prey–predator modelling. However, it sometimes becomes very difficult, if not impossible, due to the high complexity and non-linearity of ecosystems except for the modeller's insufficient understanding to the investigated processes (Recknagel, 1997). A good alternative is the application of artificial intelligence (AI) techniques (Minns, 1998) that include artificial neural networks (ANN), genetic programming (GP) and fuzzy logic (FL). These are recently more and more widely used methods, and are proved to be promising in the future. Our next research will take more efforts to the application of ANN and FL to evolution rules definition. Probably, the most promising way is to combine the AI techniques with numerical approaches, which has been demonstrated by Bokhorst and Vonk (see Passarge, 1998).

Appendix A. Model algorithms

A.1. Germination

The germination biomass from seeds are expressed by:

$$Bio\_C = CSR*CTS*CSW*CBS \tag{A1}$$

$$Bio\_P = PSR*PTS*PSW*PBS \tag{A2}$$

where Bio_C: biomass density of *C. aspera* after germination in cell; *CSR*: *C. aspera* sprout ratio; *CTS*: *C. aspera* total seeds; *CSW*: *C. aspera* seed weight; *CBS:* ratio of biomass from *C. aspera* seed.

The similar meanings also apply to Eq. (A2) for *P. pectinatus*.

A.2. Initialisation

After germination, they are initialised exponentially (Marcel, 1999) by biomass from propagules with a constant rate;

$$Bio\_C = Bio\_C*(1 + CIR)^{CID} \tag{A3}$$

Table 1
Experimental values for P_{max}, K_m and R

Species	P_{max}	K_m	R
C. aspera	4.4	2.1	−0.22
P. pectinatus	3.3	2.0	0.26

$$Bio\_P = Bio\_P*(1 + PIR)^{PID} \qquad (A4)$$

where CIR: C. aspera initialisation rate; CID: C. aspera initialisation date.

A.3. Shading

It is assumed that 100% shading is experienced when cell itself and its eight neighbours are all saturated, then the real shading coefficient is computed as:

$$SC = \sum_{i=1}^{9} (Bio\_C_i + Bio\_P_i)/((CSB + PSB)*9) \qquad (A5)$$

$$SP = \sum_{i=1}^{9} (Bio\_P_i)/((CSB + PSB)*9) \qquad (A6)$$
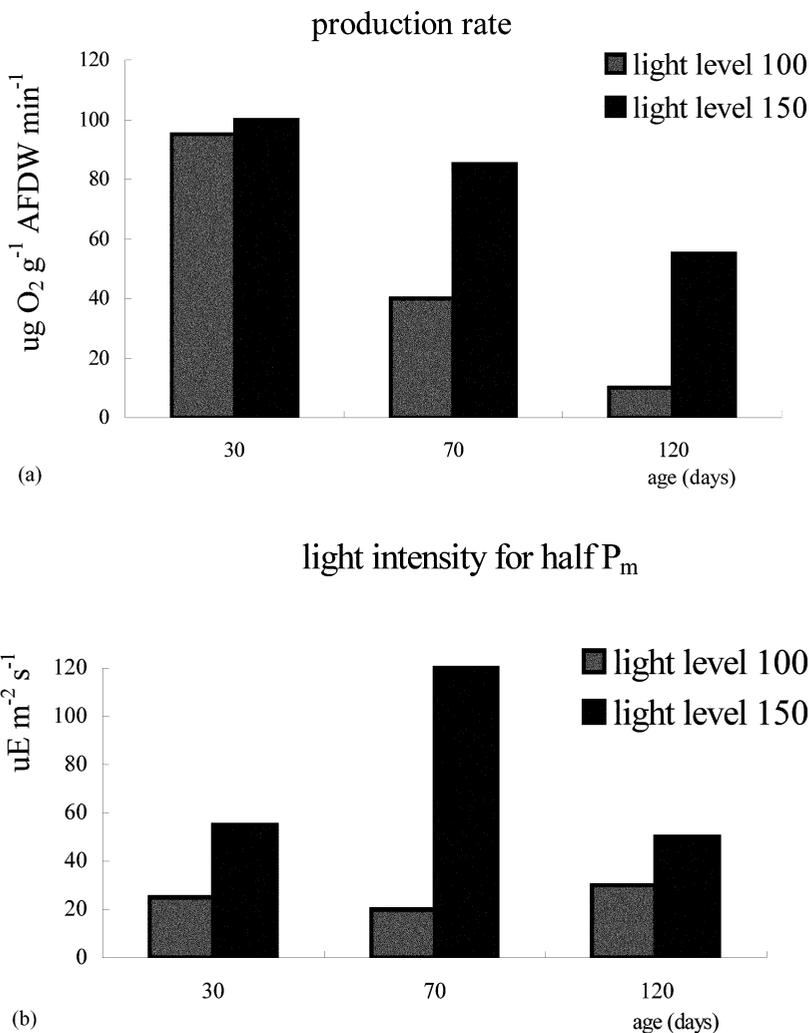
Fig. 6. (a) Max rate of gross photosynthesis. (b) Light intensity where $P_m/2$ is reached.

Table 2
Empirical values for some model parameters

Description	Name	Value for *C. aspera*	Name	Value for P.pectinatus
Cell area (m²)	Area	100	Area	100
Water depth (m)	DC	1.2	DP	0.8
Emerge time (day)	EC	25	EP	10
seed sprout ratio	CSR	15%	PSR	20%
Biomass ratio from seed	CBR	25%	PBR	25%
Seed weight (g)	CSW	0.00018	PSW	0.02
Initialisation rate	CIR	0.12	PIR	0.22
Initialise time (day)	CID	10	PID	6
Day length (h)	DL	10 (120th–150th), 14 (151th–210th), 12 (211th–240th)	DL	10 (120th–180th), 14 (151th–210th), 12 (211–240th)
Light level (µE m⁻² s⁻¹)	LL	120 (120th–150th), 180 (151st–210th), 160 (211st–240th)	LL	120 (120th–150th), 180 (151th–210th), 160 (211th–240th)
Depth averaged light Attenuation	AC	Unvegetated area 2.5/m, 2.0/m (after sprout), 1.0/m (after initialisation)	AP	Unvegetated area 2.5/m, 2.0/m (after sprout), 0.8/m (after initialisation)
K_m(µE m⁻² s⁻¹)[a]	K_m_C	Take K_m_P/3, 14.0	K_m_P	From graph 52.0
P_m(g O₂ g⁻¹ AFDW h⁻¹)[a]	P_m_C	From graph 0.11	P_m_P	From graph 0.059
O₂ conversion	*conv*	0.82	Conv	0.82
[HCO₃⁻]	[HCO₃⁻]	Unvegetated area 2.5 M, 2.5 M (120th–180th), 0.4 M (181st–240th)	[HCO₃⁻]	Unvegetated area 2.5 M, 2.5 M (120th–180th), 0.4 M (181st–240th)
Respiration rate (g O₂ g⁻¹ AFDW h⁻¹)	CRR	0.029	PRR	0.012
Respiration time (h)	RT	24	RT	24
Mortality rate	CMR	0.001	PMR	0.002
Saturation biomass	CSB	350	PSB	350
Seed yield ratio	CSYR	35%	PSYR	20%
Seed loss ratio	CSLR	20%	PSLR	20%

[a] P_m, max rate of gross photosynthesis. K_m, light intensity at which half P_m is reached.

where *SC*: is the shade effect on *Chrophyte*; *Bio_C_i*: *C. aspera* biomass in cell i; *CSB*: *C. aspera* saturated biomass.

A.4. Available light level

The available light level is the light level after shading, given by:

$$CNL = LL*(1.0 - SC) \tag{A7}$$

$$PNL = LL*(1.0 - SP) \tag{A8}$$

where *LL*: light level; *CNL*: *C. aspera* net light level; *PNL*: *P. pectinatus* net light level.

A.5. Underwater light intensity

Light intensity, which is assimilated for photo-synthesis, is computed at half depth with the effect of light attenuation as:

$$CLI = CNl*e^{-0.5*DC*AC} \tag{A9}$$

$$PLI = PNL*e^{-0.5*DP*AP} \tag{A10}$$

where *DC*: depth *C. aspera* mainly colonises; *AC*: attenuation coefficient for *C. aspera*; *CLP*: *Chrophyte* light intensity.

A.6. Coefficients of [HCO₃⁻] effect

The HCO₃⁻ factor is assumed to be 1.0 when the concentration is equal or higher than 2.5 mM, then the factor inside the vegetated area after day 181st is computed by the equation from fitted curve (Marcel, 1999)

$$CC = \frac{\dfrac{P_{max}^C * [\text{HCO}_3^-]}{K_m^C + [\text{HCO}_3^-]} - R^C}{\dfrac{P_{max}^C * 2.5}{K_m^C + 2.5} - R^C} \tag{A11}$$

$$CP = \frac{\dfrac{P_{max}^P * [\text{HCO}_3^-]}{K_m^P + [\text{HCO}_3^-]} - R^P}{\dfrac{P_{max}^P * 2.5}{K_m^P + 2.5} - R^P} \tag{A12}$$

where P_{max} = maximum photosynthesis rate; K_m = half saturation constant; R = photorespiration. The experimental values for P_{max}, K_m and R are given in Table 1.

A.7. Production

Daily biomass production in each cell is computed from daily photosynthesis (O_2 g/day) production multiplied by the conversion factor *conv*, which is expressed as:

$$PC = \frac{Bio\_C_t * (P_{m\_C} * CLI) * conv * CC * DL}{K_{m\_C} + CLI} \tag{A13}$$

$$PP = \frac{Bio\_P_t * (P_{m\_P} * PLI) * conv * CP * DL}{K_{m\_P} + PLI} \tag{A14}$$

where *PC*: the photosynthesis product of *C. aspera*; Bio_C_t: *C. aspera* biomass at time *t*; *conv*: is biomass conversion coefficient, takes value 0.82; P_{m_C}: max photosynthesis rate of *C. aspera*; K_{m_C}: light intensity where half P_{m_C} is reached; P_{m_P}: max photosynthesis rate of *P. pectinatus*, takes value from (Fig. 6b); K_{m_P}: light intensity where half P_{m_P} is reached, takes value Fig. 6a.

Since no such kind of graph is found in literature study for *C. aspera*, K_m of *C. aspera* takes one third of that of *P. pectinatus* according to the experimental result (Marcel, 1999).

A.8. Respiration loss

The respiration is proportional to the total current biomass of each cell

$$CR = Bio\_C_t * CRR * RT * conv \tag{A15}$$

$$PR = Bio\_P_t * PRR * RT * conv \tag{A16}$$

where *CR*: *C. aspera* respiration; *CRR*: *C. aspera* respiration ratio; *RT*: daily respiration time in hour.

A.9. Mortality loss

Mortality is also proportional to the total current biomass in the cell, given by:

$$CM = CMR * Bio\_C_t \tag{A17}$$

$$PM = PMR * Bio\_P_t \tag{A18}$$

where *CM*: mortality of *C. aspera*; *CMR*: *C. aspera* mortality ratio.

A.10. Resources bulk

The resources bulk of each cell is calculated by subtracting the respiration from the production, expressed by:

$$CRB = CP - CR \tag{A19}$$

$$PRB = PP - PR \tag{A20}$$

where *CRB*: *C. aspera* resources bulk.

A.11. Biomass updating of each cell

The biomass density at time $t + 1$ is then computed as:

$$Bio\_C_{t+1} = Bio\_C_t + CRB - CM \tag{A21}$$

$$Bio\_P_{t+1} = Bio\_P_t + PRB - PM \tag{A22}$$

where Bio_C_{t+1}: biomass of *C. aspera* at time $t + 1$.

A.12. Spreading

If the sum of Bio_C_{t+1} and Bio_P_{t+1} is larger than the saturated biomass, and there is space available in near neighbour, then spreading happens.

The procedures from (*A.3*) to (*A.12*) are repeated until the end of annual growth period.

A.13. Formation of seeds

The seeds yield is proportional to the biomass at the end of growth period

$$CSY = Bio\_C * CSYR/CSW \tag{A23}$$

$$PSY = Bio\_P * PSYR/PSW \tag{A24}$$

where CSY: *C. aspera* seeds yield; $CSYR$: *C. aspera* seeds yield ratio.

The total seeds available for germination are then computed by:

$$CTS = (CSY + CTSL * (1.0 - CSR)) * (1 - CSLR) \tag{A25}$$

$$PTS = (PSY + PTSL * 1.0 - PSR)) * (1 - PSLR) \tag{A26}$$

where $CTSL$: *C. aspera* total seed in last year; $CSLR$: *C. aspera* seed loss ratio in winter.

Parameters used in this model are presented in Table 2.

References

Anderson, D.M., 1995. Toxic red tides and harmful algal blooms: a practical challenge in coastal oceanography. Reviews of Geophysics, Supplement, July 1995: 1189–1200.

Babovic, V., Baretta, J., 1996. Individual based modelling of aquatic. In: Muller, A., (Ed.), Proceedings of Hydroinformatics Conference 1996, Balkema Zurich, Switzerland.

Balzter, H., Braun, P.W., Kohler, W., 1997. Cellular automata models for vegetation dynamics. Ecological Modelling 107, 113–125.

Blaine, T.W., DeAngelis, D.L., 1997. The interaction of spatial scale and predator-prey functional response. Ecological Modelling 95, 319–328.

Camara, A.S., Ferreira, F.C., Loucks, D.P., Seixas, M.J., 1990. Multidimensional simulation applied to water resources management. Water Resource Research 26, 1877–1886.

Carter, J., Finn, J.T., 1999. MOAB: a spatially explicit, individual-based expert system for creating animal foraging models. Ecological Modelling 119, 29–41.

Chapra, S.C., 1998. Engineering approaches to algal modelling and management. In: Algal Modelling: Processes and Management. Proceedings of a Conference held at University of Reading, July 1998.

Chen, C.W., Orlob, G.T., 1975. Ecological Simulation of Aquatic Environment. System Analysis and Simulation in Ecology, vol. 3. Academic Press, New York, pp. 476–588.

Dahl-Madsen, K.I., Strange-Nielsen, K., 1974. Eutrophication models for ponds. Vand 5, 24–31.

David, A., Ricard, V.S., 2000. The DivGame simulator: a stochastic cellular automata model of rainforest dynamics. Ecological Modelling 133, 131–141.

DeAngelis, D.L., Gross, L.J., 1992. Individual Based Models and Approaches in Ecology: Concepts and Models. Routledge, Chapman and Hall, New York.

DeAngelis, D.L., Godbout, L., 1991. An individual-based approach to predicting density-dependent dynamics in smallmouth bass populations. Ecological Modelling 57, 91–115.

Donaghay, P.L., Osborn, T.R., 1997. Toward a theory of biological-physical control of harmful algal bloom dynamics and impacts. Limnology and Oceanography 42, 1283–1296.

Elisabeth, H.S. van Duin, 1992. Sediment transport, light and algal growth in the Markermeer. PhD thesis, University of Wageningen.

Engelen, G., White, R., Uljee, I., 1998. Integrating constrained cellular automata models, GIS and decision support tools for urban planning and policy making. In: Timmermans, H. (Ed.), Decision Support System in Urban Planning. E&FN Spon, London.

Gronewold, A., Sonnenschein, M., 1998. Event-based modelling of ecological system with asynchronous cellular automata. Ecological Modelling 108, 37–52.

Hal, C., Ron, J.E., 1996. Ecological interactions in patchy environments: from patch-occupancy models to cellular automata. Lecture Notes in Biomathematics 94–109.

Hinckley, S., Hermann, A.J., Megrey, B.A., 1996. Development of a spatially explicit, individual-based model of marine fish early life history. Marine Ecology Progress Series 139, 47–68.

Hong, S.H., David, J.M., Joel, B., 1999. An object-oriented forest landscape model and its representation of tree species. Ecological Modelling 119, 1–19.

Hosper, S.H., 1997. Clearing Lakes. PhD thesis, Agriculture University, Wageningen, p. 168.

Jørgensen, S.E., 1976. An eutrophication model for a lake. Ecological Modelling 2, 147–165.

Jørgensen, S.E., 1994. Fundamentals of Ecological Modelling, 2nd ed. Elsevier Science, Amsterdam.

Jørgensen, S.E., 1998. A Handbook of Ecological Modelling.

Karafyllidis, I., Thanailakis, A., 1996. A model for predicting forest fire using cellular automata. Ecological Modelling 99, 87–97.

Marcel, S., 1999. Charophyte colonisation in shallow lakes. PhD thesis, University of Amsterdam.

Masahiko, S., Hiroshi, N., Ukita, M., 1991. A shallow-sea ecological model using an object-oriented programming language. Ecological Modelling 57, 221–236.

May, R.M. (Ed.), 1976. Theoretical Ecology, Principles and Applications. Blackwell Scientific, Philadelphia, PA.

McDermot, D., Rose, K.A., 2000. An individual-based model of lake fish communities: application to piscivore stocking in Lake Mendota. Ecological Modelling 125, 67–102.

Minns, A.W., 1998. Artificial Neural Network as Subsymbolic Process Descriptors. PhD Thesis, Technique University of Delft, The Netherlands.

Minns, A.W., Mynett, A.E., Chen, Q., van den Boogaard, H.F.P., 2000. A cellular automata approach to ecological modelling. In: Odgaard, A.J. (Ed.), Proceedings of Hydroinformatics Conference 2000, Iowa, USA.

Passarge, J., 1998. Harmful algal blooms-red tides. WL|delft Hydraulics Report, Z2494.

Petersen, J.H., DeAngelis, D.L., 2000. Dynamics of prey moving through a predator filed: a model of migration juvenile salmon. Mathematical Biosciences 165, 97–114.

Recknagel, F., 1997. ANNA-artificial neural networks model for predicting species abundance and succession of blue-green algae. Hydrobiologia, 349, 47–57.

Rechnagel, F., Petzoldt, T., Jaeke, O., Krusche, F., 1994. Hybrid expert system DELAQUA—a toolkit for water quality control of lakes and reservoirs. Ecological Modelling 71, 17–36.

Scheffer, M., Baveco, J.M., DeAngelis, D.L., Rose, K.A., van Nes, E.H., 1995. Super-individuals a simple solution for modelling large populations on an individual basis. Ecological Modelling 80, 161–170.

Sirakoulis, G.C.h., Karafyllidis, I., Thanailakis, A., 2000. A cellular automaton model for the effect of population movement and vaccination on epidemic propagation. Ecological Modelling 133, 209–223.

Van Nes, E.H., Scheffer, M., Van den berg, M.S., Coops, H., 1998. Charisma: a spatial, multi-species model of submerged macrophytes. Proceedings of the 10th EWRS International Symposium of Aquatic Weeds, Lisbon, pp. 211–214.

Vermij, S.G., 1987. Analysis of algal growth in Lake Maarsseveen by means of mathematical modelling. PhD thesis, University of Amsterdam.

Von Neumann, J., 1949. Theory of self-reproducing automata. In: Burks, A.W. (Ed.), University of Illinois Lectures on the Theory and Organisation of Complicated Automata. University of Illinois Press, Urbana, IL.

Wolfram, S., 1984. Computational Theory of Cellular Automata. Common. Mathematical Physics 96, 15–57.